Theory of Filamentary Plasma Array Formation in Microwave Breakdown at Near-Atmospheric Pressure

Sang Ki Nam* and John P. Verboncoeur

Department of Nuclear Engineering, University of California, Berkeley, California 94720-1730 USA

(Received 25 January 2009; published 31 July 2009)

Recently reported observations of filamentation during high power microwaves breakdown of near-atmospheric pressure gas are explained using a one-dimensional fluid model coupled to a theoretical wave-plasma model. This self-consistent treatment allows for time-dependent effects, plasma growth and diffusion, and partial absorption and reflection of waves. Simulation results, consistent with experiments, show the evolution of the plasma filaments spaced less than one-quarter wavelength, the sequential discrete light emission propagating back toward the source, and the diffusion and decay of the plasma. The model allows examination of many features not easily obtained experimentally, including dependence on field strength and frequency, pressure, and gas composition, which influence the breakdown and emission properties, including the spacing and speed of propagation of the filaments.

DOI: 10.1103/PhysRevLett.103.055004 PACS numbers: 52.80.Pi, 51.50.+v, 52.38.Hb, 52.40.Db

Plasma breakdown is a basic phenomenon of importance in many areas including fusion energy, space plasma, space propulsion, plasma processing, dusty plasma, and high power microwave (HPM) systems. In the HPM community, plasma breakdown is of great interest since it is a major limiting factor in transmission of HPM radiation. Many studies have been done on this topic in theory and experimentation [1–6]. Recently, filamentary array formation was observed during breakdown of near-atmospheric pressure gas by high power microwaves in HPM experiment and reported in this journal [7]. The initial breakdown generated the first plasma filament as a single breakdown spot by the interaction of a seed electron and an incident Gaussian microwave beam from a 1.5 MW, 110 GHz gyrotron. The sequential discrete light emission propagated back torward the gyrotron power source [8], creating a sequential discrete filamentary array. The filamentary array consisted of a number of plasma filaments regularly spaced about one-quarter wavelength apart in the plane perpendicular to the electric field direction. In [7], a model was developed by placing ideal conducting posts at the location of one or more experimentally observed filaments, and then computing the resulting fields in two dimensions. While not including the transient growth of the plasma filaments, diffusion effects, and the partial absorption and reflection of the waves, this model demonstrated that the resulting field pattern had a peak in a plane one-quarter wavelength from the filament. The development of the array was explained as a result of diffraction of the beam around the filaments leading to the sequential generation of the filaments. This hypothesis assumed that the initial filament should be able to develop plasma density high enough within a small localized spot to diffract (or reflect) the incident wave. The model does not explain why filaments developed only one-quarter wavelength upstream of existing filaments, and not at other locations where the maximum electric field also exists (e.g., three quarters wavelength upstream). The simple model also cannot explain why filaments form at distances less than one-quarter wavelength, why a diffuse plasma is sometimes formed, and the mechanism for the finite propagation speed of the filaments. Similar discrete plasma structures at lower microwave frequencies have been reported and theoretical explanations were attempted [9–12]. None of these theories, however, adequately explain the regularly spaced plasma filaments, generated by the 110 GHz microwaves. In this Letter, we propose the physical mechanisms responsible for development of the regular plasma filamentary array and develop a one-dimensional self-consistent fluid model coupled to a theoretical model of wave reflection, transmission, and absorption in an arbitrary profile plasma slab to investigate the mechanisms for plasma filament formation. Although the model cannot capture the two-dimensional nature of the filaments observed in [7], it can successfully explain the fundamental physics behind the filament spacing less than one-quarter wavelength, the propagation speed, the dependence on physical parameters including electric field, gas composition and pressure, and frequency, including transient effects including partial reflection and absorption of waves at partially formed filaments, and diffusion of the plasma.

We hypothesize that the physical mechanisms responsible for the development of the filamentary array are the reflection of incident waves by the plasma filament and ambipolar diffusion of electrons from the plasma filaments. The wave reflected at high density filaments constructively interferes with the incident wave, resulting in maximum field strength at a distance one-quarter wavelength, $\lambda/4$, upstream from the plasma filament as in Ref. [7]. Ambipolar diffusion, due to space charge effects in the high density filaments, explains why the next sequential plasma filament develops only at $\leq \lambda/4$ upstream from the filament, and not near $3\lambda/4$ where another peak of electric field exists. When electrons approach the $\leq \lambda/4$ peak in

electric field by ambipolar diffusion from the nearest filament, the strong electric field drives local ionization resulting in growth of a new plasma filament at that location. Note that strong ionization effect can occur at $<\lambda/4$ when the breakdown threshold is exceeded due to the nonlinear dependence on the plasma density. Before sufficient electrons reach the next peak at $3\lambda/4$, the new plasma filament starts to reflect the incident wave and develops a new interference pattern with the electric field peaks shifted by $\sim\lambda/4$, and the process begins again.

We developed a simple 1D model to verify our hypotheses and investigate the development of plasma filamentary arrays. The model consists of a 1D plasma fluid model and a 1D wave equation. The schematic of the simulation domain is shown in Fig. 1. Since we seek fundamental physical understanding, the gas considered in this model is argon to keep the chemistry simple. The 1D fluid model is applied for medium 2 in Fig. 1, and consists of particle continuity with a drift-diffusion approximation and an electron energy equation:

$$\begin{aligned}
\frac{\partial n_e}{\partial t} &= -\nabla\cdot J_e + K_{\text{ion}} n_e n_{\text{gas}},\\
J_e &= -D_e\nabla n_e - \mu_e n_e E_{||}, \qquad E_{||} = \frac{D_i - D_e}{\mu_i + \mu_e}\frac{\nabla n_e}{n_e},\\
\frac{\partial}{\partial t}\left(\frac{3}{2} n_e T_e\right) &= -\nabla\cdot q_e + P_{\text{abs}} - (\varepsilon_{\text{ion}} K_{\text{ion}} n_e n_{\text{gas}}\\
&\quad + \varepsilon_{\text{exc}} K_{\text{exc}} n_e n_{\text{gas}} + \tilde{K}_{\text{mom}} n_e n_{\text{gas}}),\\
q_e &= -\frac{3}{2} D_e \nabla n_e T_e + \frac{5}{2} J_e T_e,\\
P_{\text{abs}} &= \frac{e n_e}{m_e \nu_{m,e}} E_\perp^2 = \mu_e n_e E_\perp^2,
\end{aligned} \tag{1}$$

where n_e and n_{gas} are the electron and neutral argon gas densities, respectively, D_e and D_i are the diffusion coefficients, and μ_e and μ_i are the mobility of electrons and argon ions, respectively, and $E_{||}$ is the ambipolar electric field which is parallel to the direction of wave propagation. The diffusion coefficient and mobility are assumed to be spatially uniform [13]. Invoking quasineutrality, the argon ion density is assumed to equal to the electron density. T_e is the electron temperature; the electron energy distribution function is assumed Maxwellian for this simple model. ε_{ion} and ε_{exc} are the ionization and excitation threshold energies, K_{ion} and K_{exc} are the ionization and excitation rate coefficients, and $\tilde{K}_{\text{mom}}$ is the momentum energy transfer rate coefficient [14]. P_{abs} is the power deposition, $\nu_{m,e}$ is the electron momentum transfer collision frequency. $E_\perp$ is the transverse electric field of the applied plane wave, calculated by the wave equation. The electron density and temperature at the boundaries ($z = z_1 = 0$ and $z = z_2 = 4$ mm in our simulation) are linearly extrapolated from the adjacent two mesh points to minimize the effect of boundaries. The effect of the microwave magnetic field is negligible in this nonrelativistic problem since electron gyrofrequency ($\omega_{\text{ce}} \sim 10^3$) is much smaller than the microwave frequency and plasma frequency, and the gyroradius is orders larger than the domain.

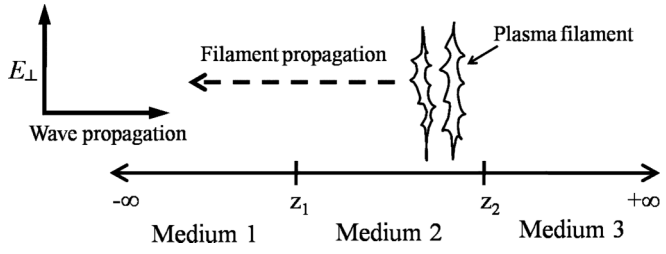

FIG. 1. The schematic of the simulation domain.

The plane wave equation for $E_\perp$ is defined by [15]:

$$\begin{aligned}
&\frac{\partial^2 Z_2}{\partial z^2} + k_{z,2}^2 Z_2 = 0,\\
&2jk_{z,1} e^{jk_{z,1}z_1} = jk_{z,1} Z_2 + \frac{\partial Z_2}{\partial z}, \quad \text{at } z = z_1,\\
&jk_{z,3}\tau = \frac{\partial Z_2}{\partial z}, \quad \text{at } z = z_2,
\end{aligned} \tag{2}$$

where Z_2 is the spatial profile of the transverse electric field as a complex function assuming a time dependence of $e^{-j\omega t}$ with the amplitude of the incident electric field of E_0, so $E_\perp$ is $\text{Re}(E_0 Z_2 e^{-j\omega t})$. Here, j is the imaginary number, and $k_{z,1}$ and $k_{z,3}$ are the wave numbers in medium 1 ($-\infty < z < z_1$) and medium 3 ($z_2 < z < +\infty$), defined by $k = \omega/c$, where ω is the angular frequency of the incident wave and c is the speed of light. $k_{z,2}$ is the complex wave number in medium 2 ($z_1 < z < z_2$), defined by

$$k_{z,2} = k_{\text{gas}}\left(1 - \sum_i \frac{\omega_{p,i}^2(z)}{\omega(\omega + j\nu_{m,i}(z))}\right)^{1/2}, \tag{3}$$

where i denotes the index of charged species, $\omega_{p,i} = (n_i q_i^2/\varepsilon_0 m_i)^{1/2}$ is the plasma frequency, and $\nu_{m,i}$ is the momentum collision frequency with the neutral gas. The boundary conditions at $z = z_1$ and $z = z_2$ are given by the continuous field conditions at the boundaries between media. For a more detailed explanation for Eq. (2), refer to Ref. [15]. In the simulation, the time step is $\Delta t = (1/f)/500$ where f is the microwave frequency ($\omega = 2\pi f$), and the uniform mesh size is $\Delta z = 0.5$ μm. The amplitude of the incident electric field is $E_0 = 5$ MV/m, the angular microwave frequency is $\omega = 110$ GHz (2.73 mm wavelength), and the pressure is $p = 760$ Torr. The fluid model and the wave equation are solved with given a field profile from the wave equation and plasma frequency from the fluid model self-consistently at every time step.

Figure 2 shows the interaction of plasma filaments with the transverse electric field. The dotted black line is the square of the transverse electric field $E_\perp^2$ averaged over one period and normalized by the value of a perfect standing wave (5×10^{13} V^2/m^2), the solid red line is the excitation rate k_{exc}, defined by $n_e K_{\text{exc}}$, averaged over one period and normalized by its maximum (1.5×10^7/sec), and the

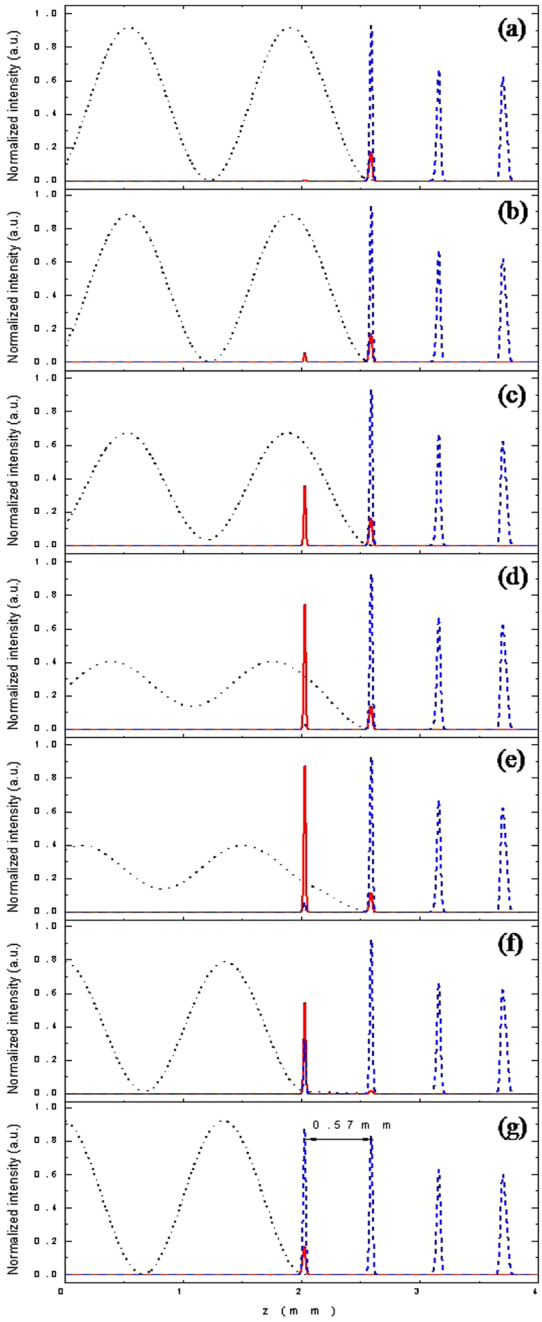

FIG. 2 (color online). Plasma filament formation at (a) $t = 6670T$, (b) $t = 6675T$, (c) $t = 6680T$, (d) $t = 6685T$, (e) $t = 6690T$, (f) $t = 6800T$, and (g) $t = 8250T$, where T is one wave period at 110 GHz. The dotted black line is the normalized square of the transverse electric field $E_\perp{}^2$, the solid red line is the normalized excitation rate k_{exc}, and the dashed blue line is the normalized electron density n_e, each averaged over one wave period.

dashed blue line is the electron density n_e averaged over one period and normalized by its maximum (4.5×10^{23} m^{-3}) in the figure. In the simulation, the location of the excitation coincides closely with the ionization. The excitation rate is plotted since the light emission which was shown in Ref. [7] is from the excitation reaction. The excitation starts at the location where the field strength is near maximum in Fig. 2(a). The field is not a perfect standing wave whose normalized maximum value is one at antinodes and minimum value is zero at nodes, but it is a quasistanding wave having a maximum value about 0.92 and a minimum value about 0.0016. The excitation grows without altering the field in Fig. 2(b). The electric field is not altered much at this time since the plasma density is not high enough yet. As the plasma filament absorbs the field, the excitation rate gets stronger in Fig. 2(c) altering the field profile, and the field is significantly disturbed and becomes far from the standing wave as the plasma density builds up in Figs. 2(d) and 2(e). Finally, the newly developed filament starts to reflect the field in Fig. 2(f) due to its high density and the field becomes a quasistanding wave again, and the ionization and excitation rates in the filament drop in Fig. 2(g). The distance between two peaks is $\sim$0.57 mm, about $0.84\lambda/4$.

Figure 2(a) is plotted again on a log scale in Fig. 3. Even though Fig. 2(a) shows only one distinct excitation peak, there are three more excitation peaks apparent in Fig. 3. These excitation peaks are not visible when they were taken by a linear intensity camera in Ref. [7] since their emission intensities are much weaker than the major excitation peak. From the simulation result, they are two to three orders smaller than the major excitation peak. Between the plasma filament peaks, Fig. 3 also shows the interfilament plasma from ambipolar diffusion, whose density is more than six orders smaller than the plasma density peak. The small density grows rapidly when it reaches the region where the breakdown electric field is exceeded. Diffusion of the fast electrons is the mechanism to supply the seed electrons for the next filament development. There is a brief transitory period during the filament growth when most of the wave is transmitted; the rapidly growing plasma frequency of the filament quickly exceeds the field frequency, causing it to become reflective. The field strength is subtly decreased after it passes the third filament

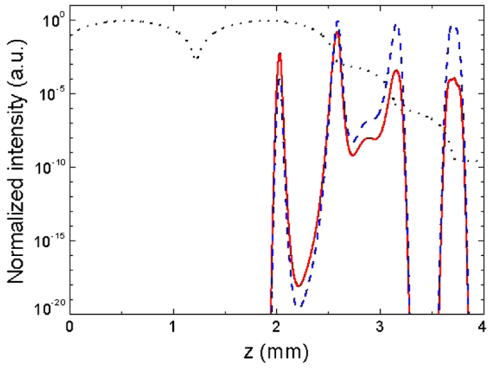

FIG. 3 (color online). Plasma filament formation in a log scale at $t = 6670T$ where T is one wave period at 110 GHz. The dotted black line is the normalized square of the transverse electric field $E_\perp{}^2$, the solid red line is the normalized excitation rate k_{exc}, and the dashed blue line is the normalized electron density n_e, each averaged over one wave period.

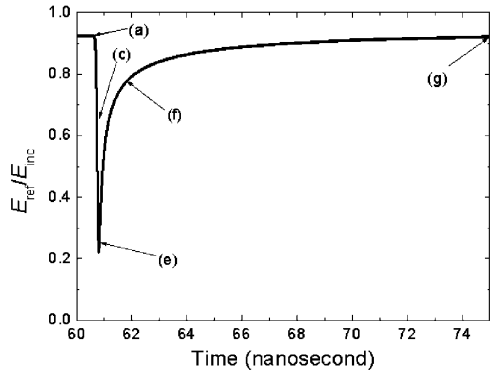

FIG. 4. Ratio of amplitude of incident electric field to reflected electric field. The timeframe corresponds to Fig. 2.

which has the maximum plasma density among the filaments. This is because the third filament absorbs and reflects most of the microwave power, and only a weak field is transmitted. Note that the plasma density should exceed $\sim 10^{20}$ m^{-3} for the plasma frequency to exceed the wave frequency, equivalent to 0.001 in the normalized plots of Fig. 2 and Fig. 3. Since most of the field is absorbed or reflected by the third filament, the second and first filaments to the right of the third filament receive insufficient microwave power to sustain the plasma density and therefore, they start to decay by diffusion.

Figure 4 shows the ratio of the amplitude of reflected to incident field, $E_{\mathrm{rec}}/E_{\mathrm{inc}}$. When the front-most plasma filament is fully developed, it reflects the incident wave and constructs the quasistanding wave which is shown having the ratio of 0.92 in Fig. 4. During this time, the plasma diffuses by ambipolar diffusion and when it reaches the location where the field is strong enough to ignite plasma breakdown, a new plasma filament starts to develop by absorbing the power. At this moment, the field starts to be altered by the filament and the ratio starts to decrease to about 0.2. During this time, the wave is far from the standing wave. As the plasma filament builds in density, the incident wave is reflected again by the front-most filament, and the ratio increases as shown in Fig. 4.

We modeled and explained the recently reported observations of the development of plasma filament arrays during breakdown of near-atmospheric pressure gas by high power microwaves using a time-dependent self-consistent one-dimensional fluid model coupled to a theoretical model of wave reflection, transmission, and absorption in an arbitrary profile plasma slab. Simulation results are consistent with experimental observation, showing the evolution of the plasma filaments spaced less than one-quarter wavelength, the sequential discrete light emission propagating back toward the source, and the diffusion and decay of the plasma. The diffusion process limits the sequential plasma filament development to less than or equal to one-quarter wavelength upstream from the previous one, where the first maximum electric field occurs. The filament rapidly builds up plasma density in a localized plane where the diffusing leading edge electrons encounter fields exceeding the breakdown threshold, rapidly forming a density peak high enough to reflect the incident wave ($\omega_{\mathrm{pe}} \gg f$), and make a quasistanding wave having the maximum field one-quarter wavelength upstream from the filament. The nonlinear breakdown and subsequent formation of a new filament occurs near the peak electric field when sufficient electrons arrive from a neighboring filament by ambipolar diffusion. The model allows examination of many features not easily obtained experimentally, including dependence on field strength and frequency, gas composition and pressure, which influence electron temperature, control the diffusion, breakdown and emission properties, and will be the subject of a future detailed examination of this phenomenon.

The authors are grateful for fruitful discussions with Y. Hidaka and R. J. Temkin. This research was supported by AFOSR Cathodes and Breakdown MURI04 Grant No. FA9550-04-1-0369.

*Author to whom correspondence should be addressed.
sang.ki.nam@berkeley.edu

[1] A. D. MacDonald, *Microwave Breakdown in Gases* (John Wiley & Sons, New York, 1966).
[2] L. Gould and L. W. Roberts, J. Appl. Phys. **27**, 1162 (1956).
[3] P. Felsenthal and J. M. Proud, Phys. Rev. **139**, A1796 (1965).
[4] J. T. Krile, A. A. Neuber, and H. G. Krompholz, Appl. Phys. Lett. **89**, 201501 (2006).
[5] John H. Booske, Phys. Plasmas **15**, 055502 (2008).
[6] S. K. Nam and J. P. Verboncoeur, Appl. Phys. Lett. **93**, 151504 (2008).
[7] Y. Hidaka, E. M. Choi, I. Mastovsky, M. A. Shapiro, J. R. Sirigiri, and R. J. Temkin, Phys. Rev. Lett. **100**, 035003 (2008).
[8] Y. Hidaka, E. M. Choi, I. Mastovsky, M. A. Shapiro, J. R. Sirigiri, R. J. Temkin, G. F. Edmiston, A. A. Neuber, and Y. Oda, Phys. Plasmas **16**, 055702 (2009).
[9] V. B. Gil'denburg and A. V. Kim, Sov. J. Plasma Phys. **6**, 496 (1980).
[10] O. A. Sinkevich and V. E. Sosnin, High Temp. **39**, 180 (2001).
[11] P. V. Vedenin and N. A. Popov, JETP **96**, 40 (2003).
[12] V. L. Bychkov, L. P. Grachev, and I. I. Isakov, Tech. Phys. **52**, 289 (2007).
[13] D. P. Lymberopoulos and D. J. Economou, J. Appl. Phys. **73**, 3668 (1993).
[14] M. A. Lieberman and A. J. Lichtenberg, *Principles of Plasma Discharges and Materials Processing* (Wiley, Hoboken, NJ, 2005).
[15] H. C. Kim and J. P. Verboncoeur, Comput. Phys. Commun. **177**, 118 (2007).